

Northward propagation of the subseasonal variability over the eastern Pacific warm pool

Xianan Jiang¹ and Duane E. Waliser¹

Received 22 February 2008; accepted 9 April 2008; published 15 May 2008.

[1] Previous studies suggest that easterly vertical shear of summer mean flow could be a key factor in the northward propagation of the subseasonal variability (SSV) over the Asian monsoon region (e.g., Jiang et al., 2004). Analysis indicates that this same mechanism may also be dictating propagation features over the eastern Pacific (EPAC). Consistent with the presence of local easterly vertical wind shear, northward propagation of the SSV is also evident over the EPAC with a phase speed of about 0.6 deg day⁻¹. Moreover, similar to its counterpart in the Indian Ocean, the northward propagating SSV over this region is also characterized by positive anomalies of equivalent barotropic vorticity and lower-tropospheric specific humidity, and planetary boundary layer (PBL) convergence, to the north of the convection center. Thus, the present study provides another independent example of the essential role that easterly vertical wind shear may be playing in regulating the meridional migration of the SSV. **Citation:** Jiang, X., and D. E. Waliser (2008), Northward propagation of the subseasonal variability over the eastern Pacific warm pool, *Geophys. Res. Lett.*, 35, L09814, doi:10.1029/2008GL033723.

1. Introduction

[2] The significant role of the subseasonal variability (SSV) for tropical climate has been widely acknowledged [e.g., Lau and Waliser, 2005; Zhang, 2005]. In addition to an eastward propagating component (i.e., Madden-Julian Oscillation (MJO)) [Madden and Julian, 1994], which is strongest in boreal winter, SSV with a period of 30–50 days is characterized by prominent northward/north–westward movement over the Indian/western Pacific Oceans during boreal summer [e.g., Yasunari, 1979; Hsu and Weng, 2001]. This meridional propagation of the SSV is found to be closely associated with active and break phases of Asian monsoon rainfall [e.g., Sikka and Gadgil, 1980; Lawrence and Webster, 2002], and thus has received significant attention over recent decades. However, current weather/climate simulation and forecast models still struggle to properly represent this form of variability [e.g., Sperber et al., 2000; Waliser et al., 2003]. Having a better understanding of this northward propagating subseasonal mode would greatly benefit a wide-range of forecasting applications [Goswami, 2005].

[3] A number of theories have been advanced in interpreting this northward propagating SSV. Webster [1983]

emphasized the important role of land surface heat flux into the planetary boundary layer (PBL) to destabilize the atmosphere north of the convection. Wang and Xie [1997] and Lawrence and Webster [2002] suggested that the northward propagation of the SSV is due to Rossby wave emanation from the eastward propagating equatorial Kelvin-Rossby wave packet. Kemball-Cook and Wang [2001] and Fu et al. [2003], on the other hand, proposed that air-sea interaction could be another factor for this northward propagation mode.

[4] Recently, based on analyses of both an atmospheric general circulation model simulation and observations, Jiang et al. [2004] identified marked meridional asymmetries in the vorticity and specific humidity fields associated with the northward propagating SSV over the Indian Ocean. A positive vorticity perturbation with an equivalent barotropic structure and maximum specific humidity are found to be located to the north of the convection center by a few degrees. By these findings, they proposed an “easterly vertical wind shear” mechanism in which the easterly vertical shear of the zonal mean flow over the Asia monsoon region (Figure 1a) could be fundamental for the northward propagation. This mechanism has also been affirmed by numerical simulations based on an intermediate model [Drbohlav and Wang, 2005, 2007].

[5] The key process associated with this mechanism is illustrated by the following equation of the barotropic component of vorticity (ζ_+), which is based on a simplified 2-D version of an intermediate model on a β -plane (the zonal variations of variables are neglected; for details please refer to Wang [2005]),

$$\frac{\partial \zeta_+}{\partial t} = -\beta v_+ - \bar{U}_T \left(\frac{\partial \omega}{\partial y} \right) \quad (1)$$

where β is the meridional variation of Coriolis parameter; v_+ is the barotropic component of meridional wind, and ω is the p-level vertical velocity. \bar{U}_T denotes the constant vertical shear of the basic zonal flow, which is defined as the difference in zonal mean wind between upper- and lower-levels. This equation indicates that in the presence of vertical easterly shear ($\bar{U}_T < 0$), positive (negative) barotropic vorticity anomalies are generated to the north (south) of the convection center due to the northward decrease (increase) of upward vertical motion associated with the subseasonal convection. The induced positive barotropic vorticity in the free atmosphere further causes a moisture convergence in the PBL due to Ekman pumping, which creates conditions that favor northward movement of enhanced rainfall. Since the Coriolis effect is involved with the Ekman pumping process, this mechanism will only be valid away from the equator and

¹Jet Propulsion Laboratory, California Institute of Technology, Pasadena, California, USA.

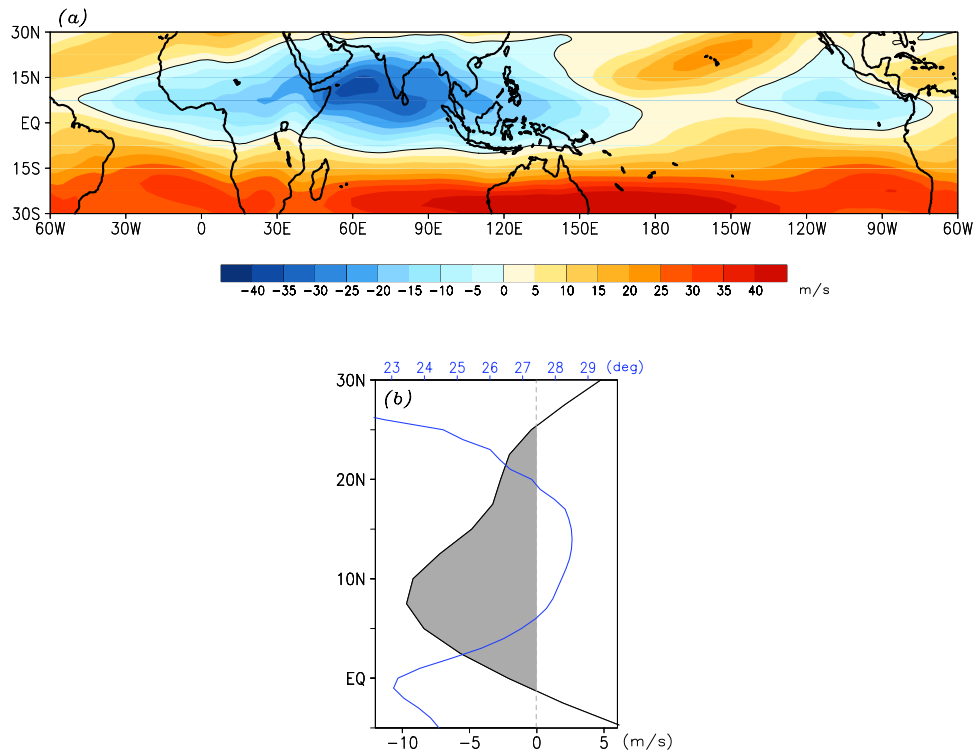


Figure 1. (a) Vertical shear of climatological summer mean (JJAS) zonal wind (200 hPa minus 850 hPa; unit: m s^{-1}) based on reanalysis-2 data set over the 1982–2005 period. (b) Meridional profiles (average over 120W–100W) of the vertical shear of the summer mean zonal wind (black curves with shading donating the easterly vertical shear; lower axis) and summer mean (JJAS) SST based on NOAA OISST v2 (1981–2006; blue curve; upper axis).

more effective with the increase of the Coriolis parameters [Jiang *et al.*, 2004].

[6] It is intriguing to note that in Figure 1a, in addition to a vast area of the Asian monsoon region, the easterly vertical shear of the summer mean flow is also evident over a small region of the eastern Pacific (EPAC). Meanwhile, the SSV of convection and winds with a period of about 40 days over the EPAC warm pool during boreal summer has been widely documented [e.g., Knutson and Weickmann, 1987; Maloney and Hartmann, 2000; Maloney and Esbensen, 2007]. These observations raise the following questions, if the easterly vertical wind shear is indeed essential for the northward propagation of the SSV, is northward propagation of the SSV evident over the EPAC? Moreover, is there similarity in the underlying thermodynamic and dynamic structures of the northward propagating SSV between this region and its counterpart in the Asian monsoon sector? The analysis in this paper seeks to address these two questions with the intention of providing an independent test of the “easterly vertical wind shear” mechanism.

2. Data and Approach

[7] A local index of the SSV over the EPAC is obtained by an extended empirical orthogonal function [EEOF] analysis of the TRMM (Tropical Rainfall Measuring Mission, version 3B42) rainfall over the EPAC warm pool (140°W–90°W; EQ–30°N). Before the EEOF analysis, 3-day mean rainfall data from January 1998 to December 2005 with horizontal resolution of 2×2 degrees are calculated based on the raw TRMM data set (0.5×0.5 degrees; daily), and are subject to

band-pass time filtering to retain the periods of 10–90 days. The EEOF is conducted with 10 temporal lags of the 3-day mean data. In order to explore the dynamic and thermodynamic structures associated with the meridional propagating SSV over the EPAC, three-dimensional daily u , v , temperature, and relative humidity are employed based on the NCAR-DOE Reanalysis-2 [Kanamitsu *et al.*, 2002] for the same period. Specific humidity is calculated based on the Clausius-Clapeyron equation by using temperature and relative humidity. To further substantiate the evidence obtained based on the reanalysis data set, shorter periods of QuikSCAT surface wind (2000–2005) and specific humidity by the Atmospheric Infrared Sounder (AIRS) [Fetzer *et al.*, 2006; Tian *et al.*, 2006] (2003–2005) are employed. All these variables are also subject to the same time filtering and 3-day mean bin averaging procedures as used for the TRMM rainfall.

3. Results

[8] The spatial pattern of EEOF₁ based on the TRMM rainfall and its associated time series are displayed in Figure 2. The EEOF₂ mode is in quadrature with the EEOF₁, and exhibits the same propagation behavior as the EEOF₁ mode. This first pair of EEOFs explains 8.1% of the total anomalous variance of 3-day average data and is well separated from other EEOFs based on North’s criterion [North *et al.*, 1982] (figure not shown). Both of them display a dominant period of 40 days based on spectral analysis of the time series. This 40-day mode is more active during boreal summer than winter (Figure 2a), which could

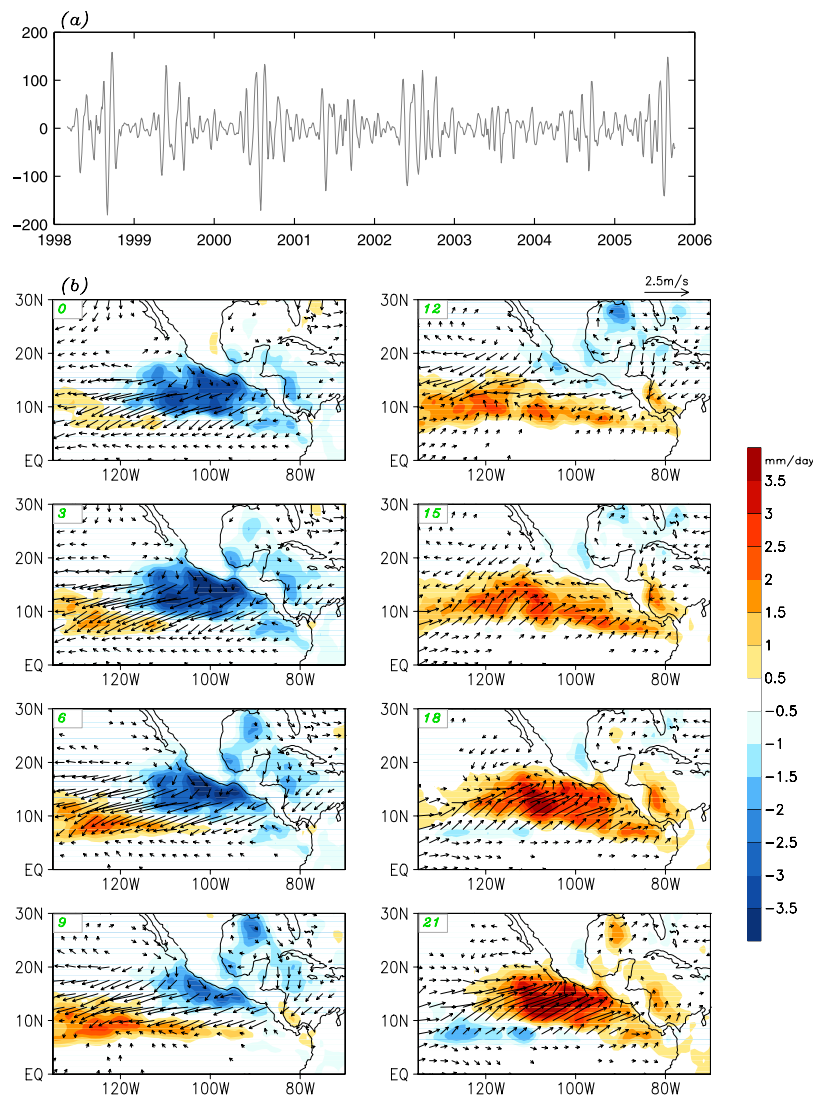


Figure 2. (a) Time series of temporal coefficients for the EEOF₁ mode. (b) Lagged regression patterns of TRMM rainfall (shaded) and QuikSCAT surface wind (vectors) versus the standardized time series of temporal coefficients for the EEOF₁ mode during boreal summer (JJAS). The time interval between adjacent panels is 3 days.

be ascribed to local cold SST in the winter due to the wind stress curl induced by strong gap winds over this region [Chelton *et al.*, 2000; Xie *et al.*, 2005]. The main features of this 40-day mode in rainfall and surface wind fields (Figure 2b) as derived by lag-regression against time series of the EOF₁ largely resemble those documented by Maloney and Esbensen [2007]. Note that a global MJO index has been employed in their study to obtain the SSV patterns in the EPAC, suggesting that the SSV over the EPAC could be a local expression of the MJO.

[9] While the eastward movement associated with this SSV has been discussed and is also clearly evident by Figure 2b, the focus here is to check the meridional migration associated with this mode. Figure 3a illustrates a Hovmöller diagram of rainfall over the longitudes of 130°W–90°W. The northward propagation of convection is readily discerned and has a phase speed of about 0.6 latitude deg day⁻¹, which is slower than that observed over the Indian Ocean (about 1 deg day⁻¹) [Jiang *et al.*, 2004]. In addition, the northward movement is generally confined between 5°N and 25°N which is largely consistent with the

region where easterly vertical shear of the mean wind is present (grey shading in Figure 1b), except for the equatorial region south of 5°N where convection is greatly suppressed due to cold SST (blue curve in Figure 1b). Note that the maximum easterly vertical wind shear is observed around 9°N, while faster northward propagation tends to occur between 10–15°N (Figure 3a). This could be explained by the stronger coupling between the mean vertical wind shear and perturbation vertical motion associated with the SSV over 10–15°N [Equation 1], given much stronger convection over these latitudes supported by local warmest SST (blue curve, Figure 1b). Moreover, as previously mentioned, more effective Ekman effect due to a larger Coriolis parameter over 10–15°N could also support stronger northward migration of the SSV than lower latitudes. In addition, the stronger easterly vertical wind shear over the Asian sector (Figure 1a) compared to the EPAC is generally consistent with the observed faster northward propagation speed over the former region.

[10] In order to examine the comprehensive evolution features associated with this subseasonal mode, regression

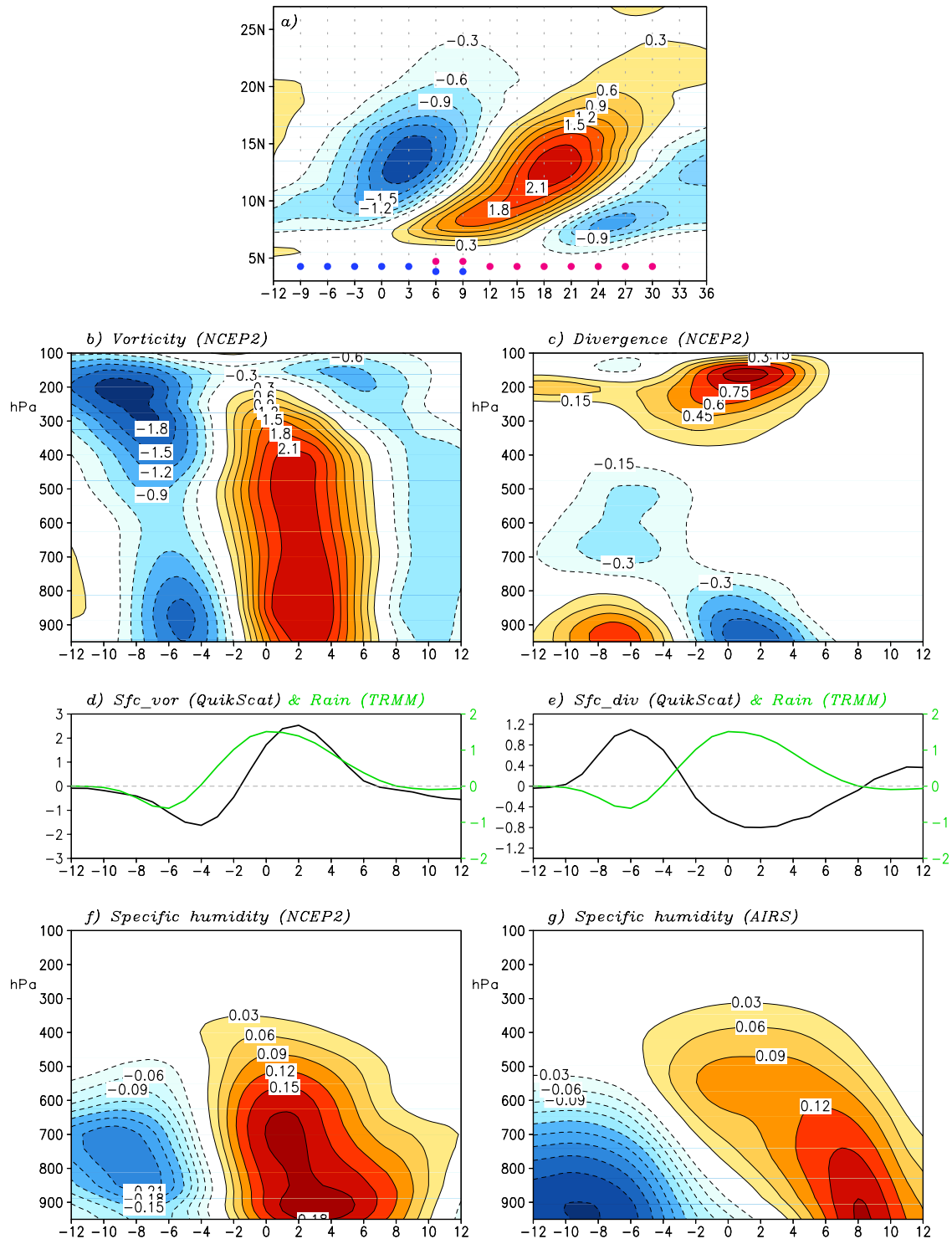


Figure 3. (a) Time-latitude distribution of rainfall perturbation (units: mm day⁻¹). Blue (red) dots show temporal points during negative (positive) rainfall phase which are employed for composite analysis to obtain meridional structures of various variables with respect to the convection center. Meridional-vertical structures of (b) vorticity (10⁻⁶ s⁻¹) and (c) divergence (10⁻⁶ s⁻¹) based on the reanalysis. (d) and (e) Black curves represent vorticity and divergence at the surface based on QuikSCAT winds (10⁻⁶ s⁻¹; left ordinates), while green curves are rainfall based on TRMM observations (mm day⁻¹; right ordinates). (f) and (g) Specific humidity structures based on the reanalysis and AIRS observations (g kg⁻¹). X-axis in Figures 3b–3g is the meridional distance (deg) with respect to the convection center. The positive (negative) value means to the north (south). All variables are averaged over longitudes between 130°W–90°W.

patterns of various variables versus the time series of the EEOF₁ mode (Figure 2a) during boreal summer (JJAS) are calculated at various lags. Similarly to Jiang *et al.* [2004], meridional structures of these variables with respect to the convection center during the northward propagation can be obtained based on a composite analysis. The temporal points used for the composite are labeled by the dots at the bottom of Figure 3a, with blue dots for the negative rainfall phase and red ones for the positive phase. At each of these temporal points, the convection center is identified; then meridional structures of vorticity, divergence, and specific humidity with respect to the convection center are averaged between 130°W and 90°W. These structures are averaged over the negative and positive rainfall phases. They are further combined together (positive phase minus negative phase) since they largely mirror each other but with an opposite sign, and are illustrated in Figures 3b–3g.

[11] It is noteworthy that the most salient features associated with the northward propagating 30–50 day SSV over the Indian Ocean, as illustrated by Jiang *et al.* [2004], are also identified with the SSV over the EPAC. In particular, a positive vorticity field with an equivalent barotropic structure is observed 2–3 degrees to the north of convection center (Figure 3b). Meanwhile, convergence in the PBL also tends to lead the convection center to the north (Figure 3c). The northward displacement of PBL convergence is largely consistent with positive equivalent barotropic vorticity perturbation, thus indicating the role of Ekman-pumping as suggested by Jiang *et al.* [2004]. The positive vorticity and PBL convergence to the north of the convection center, as identified in the reanalysis data set shown in Figures 3b and 3c, are further affirmed by the vorticity (Figure 3d) and divergence (Figure 3e) signals at the surface based on QuikSCAT observations.

[12] Moreover, as with its counterpart over Asian monsoon sector, positive specific humidity anomalies associated with northward migrating SSV over the EPAC is also found to lead the convection center, especially in the lower troposphere, based on both the reanalysis (Figure 3f) and AIRS data sets (Figure 3g). Note that differences can be evident in the humidity structures depicted by these two data sets. The northward shift of the maximum specific humidity anomaly relative to the convection center is about three degrees by the reanalysis and eight degrees by the AIRS data. The amplitude of the moisture perturbation is slightly weaker in the AIRS observations than that in the reanalysis. Also, stronger vertical tilting of the moisture field is found in the AIRS observations, with clear PBL drying near the convection center, which is not evident in the reanalysis. This PBL drying near the convection center could be associated with mesoscale downdraft processes [e.g., Kiladis *et al.*, 2005; Fu *et al.*, 2006; Tian *et al.*, 2006]. However, a period of eight years of the reanalysis data set has been employed when calculating the composite patterns, and only three years for the AIRS observations, and thus could partially be responsible for the difference in these two composite moisture fields.

4. Summary and Discussion

[13] Previous investigation indicates that easterly vertical shear of the summer mean flow may exert direct influence

on the northward propagation of the SSV over the Asian monsoon region through the “easterly vertical wind shear” mechanism. In addition to the Asian monsoon region, easterly vertical shear of the mean flow is also evident over the EPAC warm pool during boreal summer, although with relatively weaker amplitude and a smaller spatial extent. Thus, inspection of meridional migration of the SSV over the EPAC offers an excellent and independent opportunity to test this mechanism.

[14] The analysis illustrates that a clear northward propagation of the SSV is indeed evident over the EPAC warm pool. The northward movement begins around the northern edge of the cold tongue of SST ($\sim 5^{\circ}\text{N}$), and proceeds until 25°N with a phase speed around 0.6 deg day^{-1} (about 0.8 m s^{-1}). The occurrence of the northward propagation over this meridional extent is largely consistent with the presence of easterly vertical wind shear over this region, supporting the important role of the easterly vertical wind shear in the northward propagation of the SSV as was proposed for its Asian Monsoon counterpart.

[15] Moreover, it is demonstrated that similar meridional structures of a number of variables associated with the northward propagating SSV in the Indian Ocean are also evident over the EPAC. In particular, a positive vorticity with equivalent barotropic structure is found several degrees north of the convection center. Meanwhile, a northward shift of PBL convergence relative to the convection center is also evident and corresponds well to the positive vorticity, suggesting the influence of the free atmosphere on the PBL through “Ekman-pumping”. These important features in the perturbation vorticity and divergence fields, derived from the reanalysis, are further affirmed by independent evidence at the surface via Quikscat observations. Moreover, as with its counterpart over the Indian Ocean, the northward propagating SSV over the EPAC is also characterized by the northward shift of positive specific humidity to the convection center, based on both the reanalysis data set and recent AIRS observations, although differences in the moisture fields based on these two data sets are discernible.

[16] Since characteristics of the northward movement of the SSV as well as its associated asymmetric structures in the dynamic and thermodynamic fields over the Indian/Pacific sectors and EPAC exhibit great similarity, the result in this study indicates that internal atmospheric dynamics may play a key role in organizing the meridional migrating SSV. It is also noteworthy that, similar to its counterpart over the Asian sector, coherent SSV in SST is also observed in association with the northward propagating convection signal over the EPAC, with suppressed (enhanced) rainfall perturbation leading positive (negative) SST anomalies by 7–10 days [Maloney *et al.*, 2008]. Further investigation is warranted to quantify the relative roles of internal dynamics versus air-sea interaction in contributing to the northward propagation of subseasonal convection over the EPAC. Since the SSV over the EPAC exerts significant influences on regional climate features, such as tropical cyclone genesis, easterly wave activity, as well as surge events over the Gulf of California associated with the North American monsoon variability [e.g., Lorenz and Hartmann, 2006], improved understanding of the SSV over this region would greatly benefit climate prediction for North and Central America.

[17] **Acknowledgments.** We are indebted to G. Kiladis, E. Maloney, X. Fu, and E. Fetzer for their valuable discussions. The TRMM 3B42 rainfall and the AIRS water vapor data sets were processed and provided by B. Tian. We also thank anonymous reviewers for their insightful comments, which lead to considerable improvements of this manuscript. This research was carried out at the Jet Propulsion Laboratory (JPL), Caltech, under a contract with NASA. X. Jiang and D. Waliser were jointly supported by the Research and Technology Development program and Human Resources Development Fund at JPL, as well as the NASA MAP and NEWS programs.

References

- Chelton, D. B., M. H. Freilich, and S. N. Esbensen (2000), Satellite observations of the wind jets off the Pacific coast of Central America. Part I: Case studies and statistical characteristics, *Mon. Weather Rev.*, *128*, 1993–2018.
- Drbohlav, H.-K. L., and B. Wang (2005), Mechanism of the northward-propagating intraseasonal oscillation: Insights from a zonally symmetric model, *J. Clim.*, *18*, 952–972.
- Drbohlav, H.-K. L., and B. Wang (2007), Horizontal and vertical structures of the northward-propagating intraseasonal oscillation in the South Asian Monsoon region simulated by an intermediate model, *J. Clim.*, *20*, 4278–4286.
- Fetzer, E. J., B. H. Lambriksen, A. Eldering, H. H. Aumann, and M. T. Chahine (2006), Biases in total precipitable water vapor climatologies from Atmospheric Infrared Sounder and Advanced Microwave Scanning Radiometer, *J. Geophys. Res.*, *111*, D09S16, doi:10.1029/2005JD006598.
- Fu, X., B. Wang, T. Li, and J. P. McCreary (2003), Coupling between northward-propagating, intraseasonal oscillations and sea surface temperature in the Indian Ocean, *J. Atmos. Sci.*, *60*, 1733–1753.
- Fu, X., B. Wang, and L. Tao (2006), Satellite data reveal the 3-D moisture structure of tropical intraseasonal oscillation and its coupling with underlying ocean, *Geophys. Res. Lett.*, *33*, L03705, doi:10.1029/2005GL025074.
- Goswami, B. N. (2005), South Asian Monsoon, in *Intraseasonal Variability in the Atmosphere-Ocean System*, edited by K. M. Lau and D. E. Waliser, pp. 19–61, Springer, Heidelberg, Germany.
- Hsu, H.-H., and C.-H. Weng (2001), Northwestward propagation of the intraseasonal oscillation in the western North Pacific during the boreal summer: Structure and mechanism, *J. Clim.*, *14*, 3834–3850.
- Jiang, X., T. Li, and B. Wang (2004), Structures and mechanisms of the northward propagating boreal summer intraseasonal oscillation, *J. Clim.*, *17*, 1022–1039.
- Kanamitsu, M., et al. (2002), NCEP-DOE AMIP-II Reanalysis (R2), *Bull. Am. Meteorol. Soc.*, *83*, 1631–1643.
- Kemball-Cook, S., and B. Wang (2001), Equatorial waves and air-sea interaction in the boreal summer intraseasonal oscillation, *J. Clim.*, *14*, 2923–2942.
- Kiladis, G. N., K. H. Straub, and P. T. Haertel (2005), Zonal and vertical structure of the Madden-Julian Oscillation, *J. Atmos. Sci.*, *62*, 2790–2809.
- Knutson, T. R., and K. M. Weickmann (1987), 30–60 day atmospheric circulations: Composite life cycles of convection and circulation anomalies, *Mon. Weather Rev.*, *115*, 1407–1436.
- Lau, W. K. M., and D. E. Waliser (Eds.) (2005), *Intraseasonal Variability of the Atmosphere-Ocean Climate System*, 474 pp., Springer, Heidelberg, Germany.
- Lawrence, D. M., and P. J. Webster (2002), The boreal summer intraseasonal oscillation: Relationship between northward and eastward movement of convection, *J. Atmos. Sci.*, *59*, 1593–1606.
- Lorenz, D. J., and D. L. Hartmann (2006), The effect of the MJO on the North American monsoon, *J. Clim.*, *19*, 333–343.
- Madden, R. A., and P. R. Julian (1994), Observations of the 40–50 day tropical oscillation—A review, *Mon. Weather Rev.*, *122*, 814–837.
- Maloney, E. D., and S. K. Esbensen (2007), Satellite and buoy observations of boreal summer intraseasonal variability in the tropical northeast Pacific, *Mon. Weather Rev.*, *135*, 3–19.
- Maloney, E. D., and D. L. Hartmann (2000), Modulation of eastern North Pacific hurricanes by the Madden-Julian Oscillation, *J. Clim.*, *13*, 1451–1460.
- Maloney, E. D., D. B. Chelton, and S. K. Esbensen (2008), Subseasonal SST variability in the tropical eastern North Pacific during boreal summer, *J. Clim.*, in press.
- North, G. R., T. L. Bell, R. F. Calahan, and F. J. Moeng (1982), Sampling errors in the estimation of empirical orthogonal functions, *Mon. Weather Rev.*, *110*, 699–706.
- Sikka, D. R., and S. Gadgil (1980), On the maximum cloud zone and the ITCZ over Indian longitudes during the southwest monsoon, *Mon. Weather Rev.*, *108*, 1840–1853.
- Sperber, K. R., J. M. Slingo, and H. Annamalai (2000), Predictability and the relationship between subseasonal and interannual variability during the Asian Summer Monsoon, *Q. J. R. Meteorol. Soc.*, *126*, 2545–2574.
- Tian, B., D. E. Waliser, E. Fetzer, B. Lambriksen, Y. Yung, and B. Wang (2006), Vertical moist thermodynamic structure and spatial-temporal evolution of the Madden-Julian Oscillation in Atmospheric Infrared Sounder observations, *J. Atmos. Sci.*, *63*, 2462–2485.
- Waliser, D. E., et al. (2003), AGCM simulations of intraseasonal variability associated with the Asian Summer Monsoon, *Clim. Dyn.*, *21*, 423–446.
- Wang, B. (2005), Theory, in *Intraseasonal Variability in the Atmosphere-Ocean System*, edited by K. M. Lau and D. E. Waliser, pp. 19–61, Springer, Heidelberg, Germany.
- Wang, B., and X. Xie (1997), A model for the boreal summer intraseasonal oscillation, *J. Atmos. Sci.*, *54*, 72–86.
- Webster, P. J. (1983), Mechanisms of low-frequency variability: Surface hydrological effects, *J. Atmos. Sci.*, *40*, 2110–2124.
- Xie, S.-P., H. Xu, W. S. Kessler, and M. Nonaka (2005), Air-sea interaction over the eastern Pacific warm pool: Gap winds, thermocline dome, and atmospheric convection, *J. Clim.*, *19*, 5–20.
- Yasunari, T. (1979), Cloudiness fluctuations associated with the Northern Hemisphere summer monsoon, *J. Meteorol. Soc. Jpn.*, *57*, 227–242.
- Zhang, C. (2005), The Madden-Julian Oscillation, *Rev. Geophys.*, *43*, RG2003, doi:10.1029/2004RG000158.

X. Jiang and D. E. Waliser, Jet Propulsion Laboratory, California Institute of Technology, MS-183-501, Pasadena, CA 91109, USA. (xianan@caltech.edu)